

# Antarctic icequakes triggered by the 2010 Maule earthquake in Chile

Zhigang Peng<sup>1\*</sup>, Jacob I. Walter<sup>1†</sup>, Richard C. Aster<sup>2</sup>, Andrew Nyblade<sup>3</sup>, Douglas A. Wiens<sup>4</sup> and Sridhar Anandakrishnan<sup>3</sup>

**Seismic waves from distant, large earthquakes can almost instantaneously trigger shallow micro-earthquakes and deep tectonic tremor as they pass through Earth's crust<sup>1</sup>. Such remotely triggered seismic activity mostly occurs in tectonically active regions. Triggered seismicity is generally considered to reflect shear failure on critically stressed fault planes and is thought to be driven by dynamic stress perturbations from both Love and Rayleigh types of surface seismic wave<sup>2</sup>. Here we analyse seismic data from Antarctica in the six hours leading up to and following the 2010  $M_w$  8.8 Maule earthquake in Chile. We identify many high-frequency seismic signals during the passage of the Rayleigh waves generated by the Maule earthquake, and interpret them as small icequakes triggered by the Rayleigh waves. The source locations of these triggered icequakes are difficult to determine owing to sparse seismic network coverage, but the triggered events generate surface waves, so are probably formed by near-surface sources. Our observations are consistent with tensile fracturing of near-surface ice or other brittle fracture events caused by changes in volumetric strain as the high-amplitude Rayleigh waves passed through. We conclude that cryospheric systems can be sensitive to large distant earthquakes.**

Sudden acceleration of ice in glaciers, icebergs and ice sheets can generate seismicity that has been associated with a variety of cryospheric processes, including crevasse opening, basal stick-slip motion, calving of terminus ice, and collisions of floating ice bodies with each other and with the ocean floor<sup>3–6</sup>. Detailed investigation of such processes is often difficult owing to harsh and/or dangerous environmental conditions and significant logistical expenditures necessary to operate in polar regions. In recent years, a new generation of geodetic and seismic instrumentation has been deployed near and atop the Antarctic and Greenland ice sheets (for example, the POLENET/AGAP and GNET/GLISN projects, respectively). These new projects are providing critical infrastructure needed to address fundamental questions about both crustal-scale tectonic structures and ice sheets, and their interactions.

Recent work<sup>4,7–9</sup> indicates that the Antarctic cryosphere may be appreciably sensitive to remote influences arising from ocean gravity waves propagating at great distances. In addition, relatively small stress changes from ocean tides are capable of modulating stick-slip behaviours at the base of ice sheet<sup>5</sup>. However, it has not yet been documented whether and how glacial dynamics might be affected

more generally by transient dynamic perturbations from surface waves of large distant earthquakes.

The 2010  $M_w$  8.8 Maule, Chile earthquake is the largest earthquake to occur in the Southern Hemisphere since the 1960  $M_w$  9.5 Chile earthquake. Owing to its enormous size, the 2010 mainshock triggered shallow earthquakes and deep tectonic tremor in North America<sup>10,11</sup> and elsewhere<sup>12</sup>. Here we conducted a systematic search of dynamically triggered seismic events in Antarctica following the Maule earthquake (Fig. 1). As in previous studies<sup>13</sup>, we applied a 5 Hz high-pass filter to all broadband recordings, and identified stations that recorded high-frequency (~5–20 Hz) events during the arrival of large-amplitude seismic waves. We used an automatic picking algorithm to identify all possible bursts that occurred within 6 h before and after the Maule mainshock. We then compared the observed and predicted bursts during the surface waves of the Maule mainshock (Supplementary Fig. 1), and confirmed the triggering significance with a statistical parameter (Supplementary Methods and Supplementary Fig. 1). We also visually examined the records to rule out any possibility that high-frequency signals could be caused by unusually noisy channels, clipping (that is, exceeding the maximum seismograph amplitude), or other nonlinear instrumental noise. Out of the 42 Antarctic stations examined, 12 (29%) of them showed clear evidence of increase in high-frequency signals during the surface-wave arrivals (Fig. 1).

Most of the high-frequency signals occurred during and immediately after the passage of long-period Rayleigh waves (Supplementary Fig. 2). This is in marked contrast with micro-earthquakes and tremor in other tectonically active regions<sup>1,2,10–13</sup> that have been observed to occur both during the Love and Rayleigh waves (Supplementary Fig. 3). The triggered signals showed diverse patterns, including very short duration (for example, less than 2 s) high-frequency bursts (for example, station HOWD; Fig. 2a–c), as well as relatively longer duration, dispersive (for example, stations AGO1, N100 and LONW, Fig. 2d–f and Supplementary Figs 4 and 5) and non-dispersive signals (for example, stations DEVL and SILY; Supplementary Figs 6 and 7).

The clearest evidence of discrete high-frequency signals was observed at station HOWD near the Howard Nunataks (Fig. 1), which is a group of ridges at the northwest corner of the Ellsworth Mountains<sup>14</sup>. Burst-like seismic signals occurred during the passage of the teleseismic P wave, and by the subsequent Rayleigh wave (Fig. 2; see also supplementary Movie 1). In addition, the events

<sup>1</sup>School of Earth and Atmospheric Sciences, Georgia Institute of Technology, Atlanta, Georgia 30332, USA, <sup>2</sup>Geosciences Department, Colorado State University, Fort Collins, Colorado 80523, USA, <sup>3</sup>Department of Geosciences, Pennsylvania State University, University Park, Pennsylvania 16802, USA, <sup>4</sup>Department of Earth and Planetary Sciences, Washington University, St Louis, Missouri 63130, USA. <sup>†</sup>Present address: Institute for Geophysics, University of Texas at Austin, 78758, USA. \*e-mail: zpeng@gatech.edu

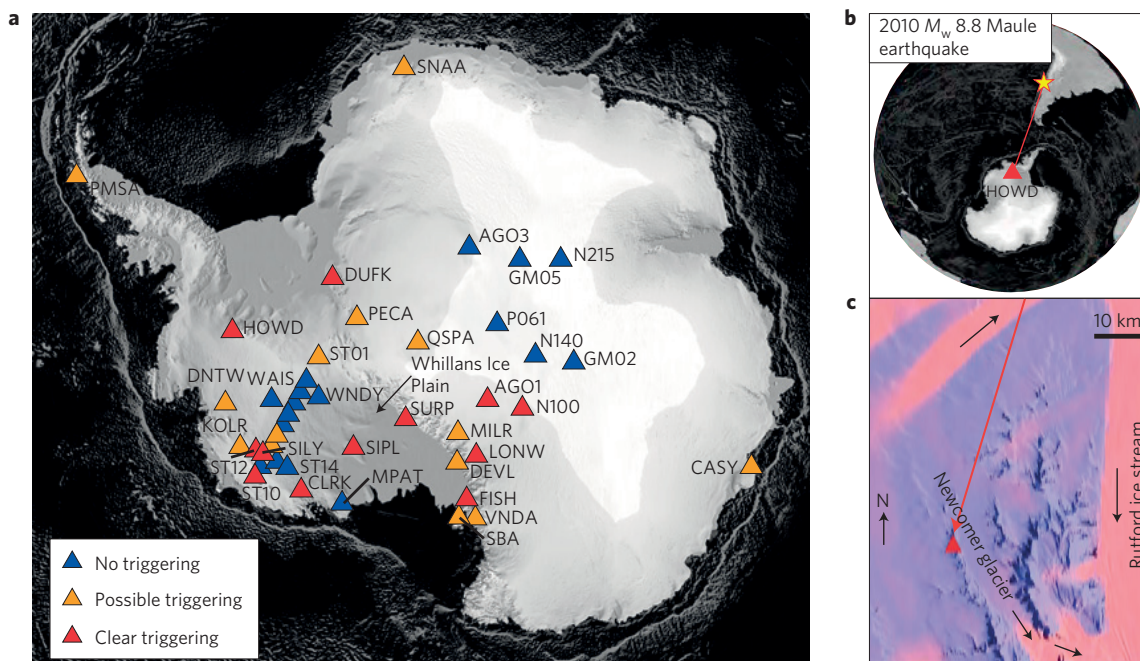


**Figure 1 | The study region in Antarctica and station HOWD, which exhibited the clearest triggering signal.** **a**, Map of Antarctica and surrounding regions indicating seismic stations where triggering clearly occurs (red), some signals may be present but status is ambiguous (orange), and no triggering observed (blue) during the passage of Maule mainshock surface waves. **b**, The great circle path ( $\sim 4,691$  km) for seismic waves from the earthquake (star) to station HOWD in the Ellsworth Mountains, Antarctica. **c**, A portion of the Landsat Image Mosaic of Antarctica<sup>24</sup>. Ice flow speed<sup>25</sup> adjacent to station HOWD (red triangle), where faster-flowing ice ( $> 50$  km  $\text{yr}^{-1}$ ) is indicated by red shading and ice that is not flowing is blue. The red arrow indicates the back-azimuth of the incoming seismic waves from the Maule mainshock.

occurred when the Rayleigh wave displacement was in the upward direction (Fig. 2c), consistent with maximal dilatational strain<sup>15,16</sup>.

We found that the triggered events at station HOWD show very high waveform similarities to each other (Fig. 3), reflecting similar repeated failure at a single source, or within a tight cluster source. The stacked waveforms (Fig. 3) do not show clear P and S arrivals with linear polarization directions, suggesting that they are probably surface waves produced by a shallow source. Further confirmation of a shallow source is indicated by a Rayleigh wave polarization analysis on the repeating bursts (see Supplementary Methods and Supplementary Figs 9 and 10), suggesting a relatively stable receiver-to-source azimuth of  $239^\circ \pm 19^\circ$ . The identification of such seismic signals as Rayleigh waves is consistent with a source very close to the surface<sup>17</sup>.

We also stacked waveforms of triggered events, and used them as templates to scan through the seismic data<sup>18</sup> six hours before and after the Maule mainshock. Although burst-like signals occurred before and after the passage of the mainshock surface waves, they do not show similar waveforms to those during the P and Rayleigh waves of the Maule mainshock (Fig. 3b). Hence, these signals probably represent background activity occurring in a different and potentially larger source volume. We also use the same template event to scan a 30-day time window around the mainshock but failed to identify any detection (Supplementary Fig. 8), suggesting that dynamic stresses from the mainshock seismic waves triggered brittle-failure events in a new region.

Figure 2 and Supplementary Fig. 4 show additional evidence of high-frequency signals triggered at stations AGO1 and N100 in East Antarctica. In both cases, the high-frequency signals were triggered during the Rayleigh waves, and had longer durations than those observed at station HOWD. Polarization analysis also reveals that most of the signals are Rayleigh waves from near-surface waves (see Supplementary Methods and Supplementary Fig. 11). These triggered events are very similar to those cryoseismic events

observed in East Antarctica<sup>19</sup>. Both showed dispersive Rayleigh waves in the frequency range of 1–8 Hz (Supplementary Fig. 12; see also Supplementary Movies 2 and 3) and can propagate several hundred kilometers across the ice sheet.

In addition to these stations, high-frequency signals observed at stations LONW and DEVL (Supplementary Figs 5 and 6) also have relatively long durations, but they are not as dispersive as stations AGO1 and N100. Although we did not observe discrete and coherent events across all 4 regional stations (AGO1, N100, LONW and DEVL) simultaneously (Supplementary Fig. 13), polarization at stations AGO1 and N100 indicates azimuths pointing to a region central to these two stations (Supplementary Fig. 14). This probably represents two scenarios: the same signal could have reached all stations, but was not clearly recorded owing to complex path effects and/or site conditions, or, there are separate triggered events across a broader region, yet only observed at 1–2 stations. The current data do not allow us to differentiate between these two scenarios.

Finally, another region that indicated clear triggering on a number of stations was identified near SILEY (Supplementary Fig. 7). Other nearby stations also recorded similar signals, although station SILEY recorded the best triggering signal in that area (Supplementary Figs 15 and 16). This is near a region that shows deep long-period earthquakes (with maximum spectral amplitude at 2–4 Hz) associated with sub-ice magmatism<sup>20</sup>, but the triggered signals observed here contain much higher frequencies, up to 15 Hz and are thus not deep long-period magmatic earthquakes.

As HOWD shows the clearest evidence for triggering, we also examined three additional teleseismic events that have produced significant dynamic stresses (for example,  $> 1$  kPa) at the study region (Supplementary Fig. 17). An earthquake signal, possibly tectonic, with clear P and S waves (S–P time of  $\sim 13$  s) occurred during the surface wave of the 2009  $M_w$  7.8 New Zealand earthquake (Supplementary Figs 18 and 19). Although some high-frequency signals occurred during the teleseismic waves of the 2011  $M_w$  9.1

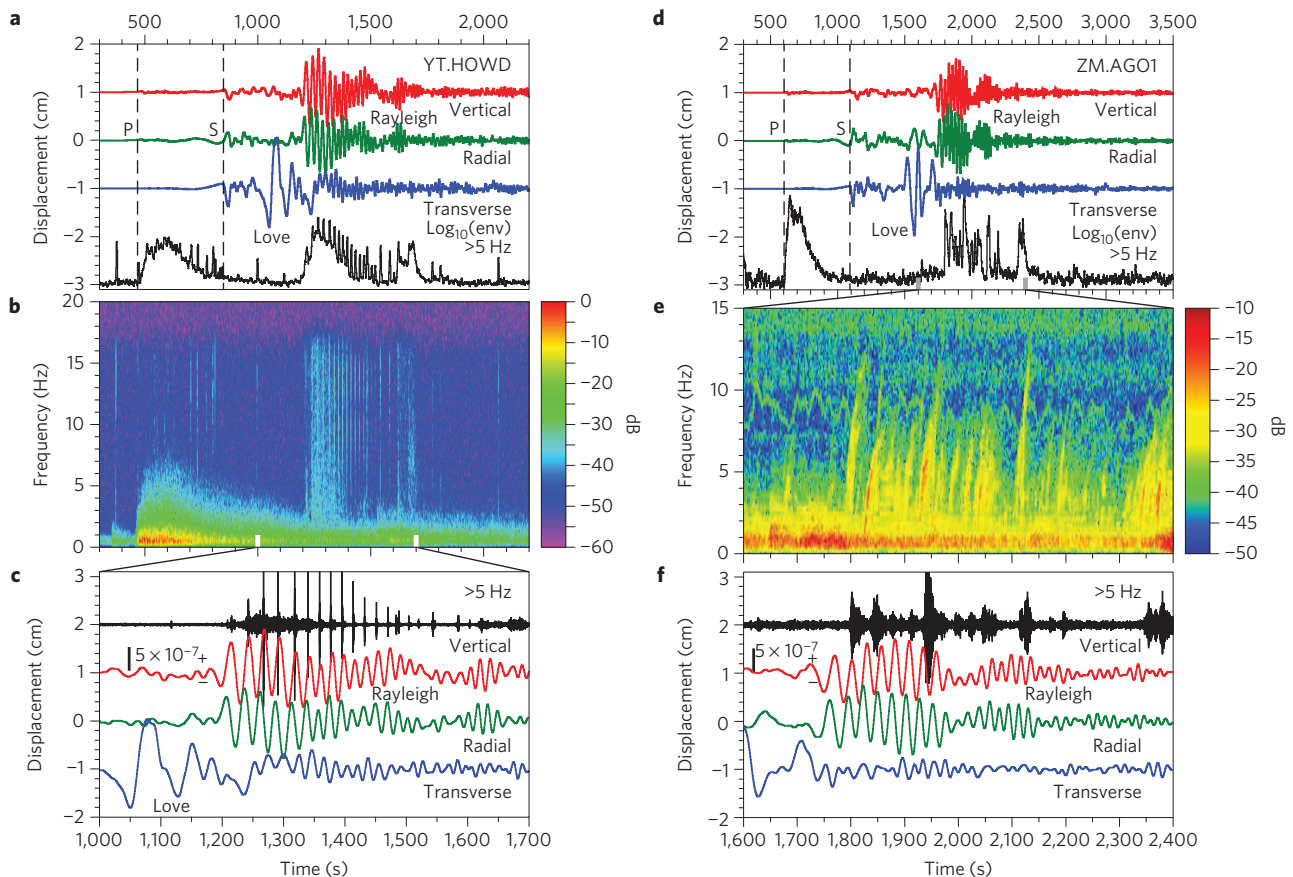


**Figure 2** | Seismic data recorded at stations HOWD and AGO1 during the 2010  $M_w$  8.8 Maule, Chile earthquake. **a**, A comparison of the three-component displacement seismograms and the 5-Hz high-pass-filtered envelope function (log-based-10) at station HOWD during the Maule mainshock. Vertical dashed lines show the predicted arrival time of P and S phases. **b**, The corresponding spectrogram for the vertical component, computed after applying a 0.5 Hz high-pass filter to suppress high-frequency artefacts from short windows<sup>26</sup>. **c**, A zoom-in plot showing the broadband displacement and the high-frequency signals during the upward motion (dilatation) of the vertical displacement. The vertical bar shows the scale for the corresponding volumetric changes. **d-f**, The same plots as for **a-c** for seismic data recorded at station AGO1.

Tohoku-Oki earthquake (Supplementary Fig. 18), they were not well modulated by the surface waves, and similar high-frequency signals also occurred before the mainshock. These observations suggest that icequakes observed after the Maule earthquake at HOWD were triggered by a higher level of dynamic stress (at least 10 kPa) and/or possibly require certain azimuths for the incoming seismic waves.

Figure 1a shows the spatial distribution of the sites that observed triggered high-frequency signals during the Maule mainshock. A general pattern is that stations in interior East Antarctica do not show any evidence of triggered high-frequency signals during surface waves (Supplementary Fig. 20). On the other hand, stations near the bedrock outcrops or near the onset regions of faster flow features (that is, ice streams or outlet glaciers) have qualitatively clearer triggering evidence by the Maule event.

As most high-frequency signals were recorded only on a single station, it is difficult to determine the source locations and their physical mechanisms. One plausible mechanism for triggering the icequakes is promoting basal slip of the ice sheet. For example, the Rutford Ice Stream is approximately 35 km from station HOWD and previous observations suggest that basal micro-earthquakes occur up to hundreds of times per hour<sup>21</sup>. However, observed events from that study showed clear P and S waves, as expected for events near the ice sheet base<sup>17</sup>. In our case, most of the observed signals are dominated by Rayleigh waves and thus consistent with

near-surface sources. In addition, if basal shear slip were responsible for generating these high-frequency burst signals, we would expect a similar and perhaps higher level of triggering during the S and Love wave, which generally produce higher shear stress changes<sup>22</sup>. The fact that Rayleigh waves, instead of Love waves, trigger the events, suggests that the high-frequency sources preferentially respond to volumetric rather than shear stress changes.

We propose a seismogenic mechanism controlled by tensile fracturing of ice in the near surface<sup>17</sup>. This is also consistent with spatial distributions of the triggering sites near the bedrock outcrops or near the onset region of ice streams, where horizontal and/or boundary effects cause high lateral stresses within the ice that form crevasses. Complicating this hypothesis is the observation that not all stations near bedrock or fast-moving glaciers show evidence of triggering (Fig. 1) and not all teleseismic earthquakes trigger events on the same site (Supplementary Fig. 17). This suggests that the sites may need to be critically stressed, or that the external stress perturbations need to exceed a threshold to produce triggering. Alternatively, we cannot completely rule out the possibility that some high-frequency signals could be produced by rock or ice falls, at least for those stations that are close to bedrock outcrops. In any case, these mechanisms would be in marked contrast with the predominant shear failure for triggered earthquakes and tectonic tremor around active plate-boundary regions<sup>1</sup>.

It is not yet clear whether icequake dynamic triggering from large distant earthquakes is ubiquitous and whether those triggered

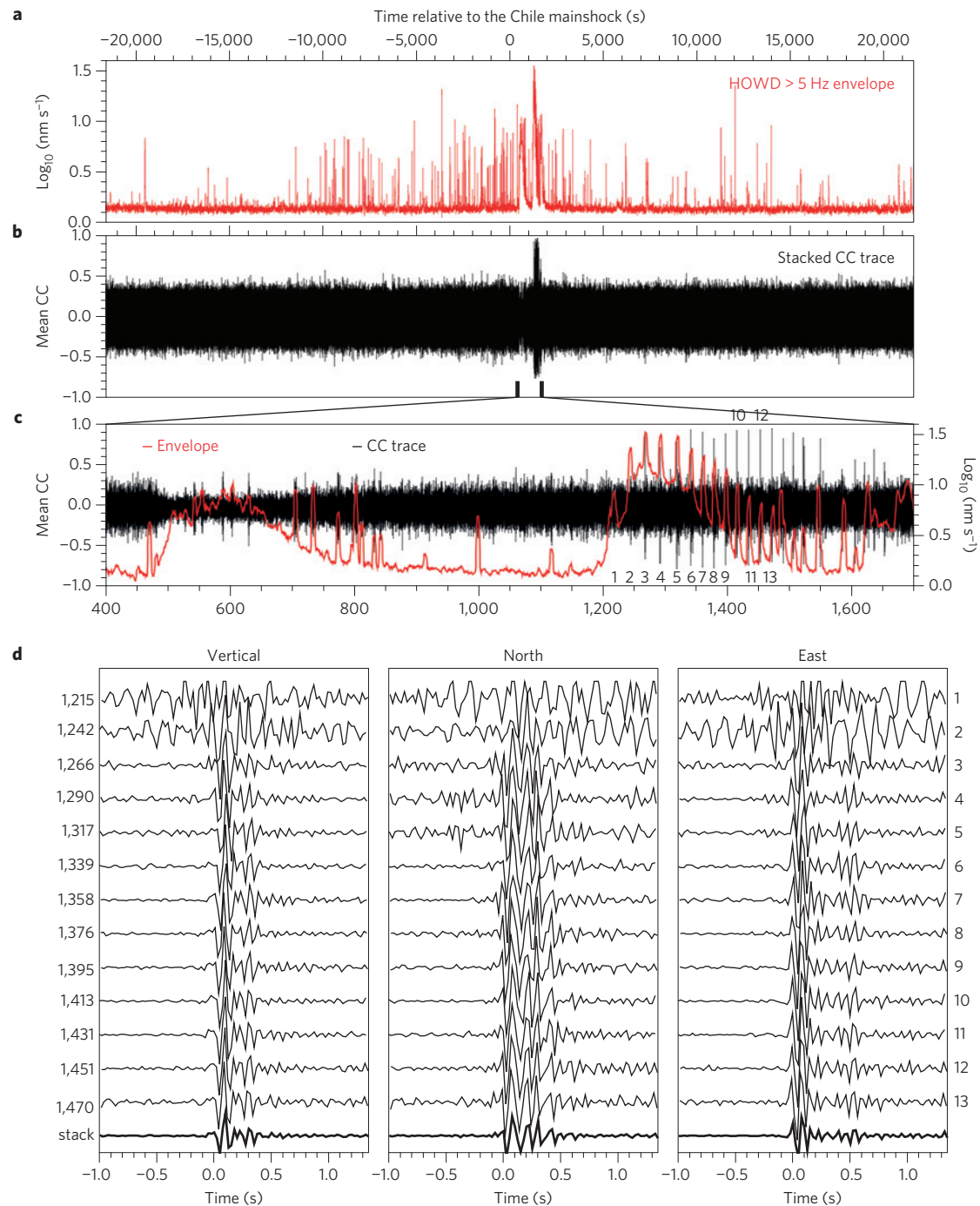


**Figure 3** | Seismic data recorded before/after the Maule mainshock and detections of high-frequency signals. **a**, 5-Hz high-pass-filtered log-based-10 envelope function showing seismic signals 6 h before and after the Maule mainshock. **b**, Mean correlation coefficient (CC) values by using the stacked high-frequency bursts during the Rayleigh wave as templates. **c**, A zoom-in plot showing a comparison between the envelope function and the CC values around the arrival time of the teleseismic waves. Numbers 1–13 mark the high-frequency bursts with waveforms shown in **d**. **d**, Individual three-component seismograms at station HOWD showing the first 13 high-frequency bursts triggered during the Rayleigh waves. The bottom traces are the stacked seismograms from bursts 3 to 13. The numbers on the left and right side mark the arrival time of the 13 bursts and their sequential numbers, respectively.

seismic signals may reflect a sudden change of nearby glacier flow, the activation of crevassing, or other related processes. A separate study<sup>23</sup> found clear evidence of glacier stick–slip motion on the Whillans Ice Plain triggered by distant earthquakes. Unfortunately, there were no available seismic data to confirm whether similar high-frequency seismic signals occurred during those triggered stick–slip events. Nevertheless, this study is emblematic of how

increasing investments in geophysical infrastructure in the polar regions are advancing our knowledge of transient processes such as basal stick–slip, calving, icequakes, and other short-duration processes. A systematic investigation of the triggerability of icequakes could lead to a better understanding of the stress state of those systems while further illuminating teleconnections and interactions between the solid Earth and cryosphere.

Received 4 January 2014; accepted 27 June 2014;  
published online 10 August 2014

## References

- Peng, Z. & Gomberg, J. An integrative perspective of coupled seismic and aseismic slow slip phenomena. *Nature Geosci.* **3**, 599–607 (2010).
- Hill, D. P. & Prejean, S. in *Earthquake Seismology* (eds Beroza, G. & Kanamori, H.) Ch. 78, 1–32 (Treatise on Geophysics Series 2nd edn, Vol. 4, in the press, 2014).
- Nettles, M. & Ekström, G. Glacial earthquakes in Greenland and Antarctica. *Ann. Rev. Earth Planet. Sci.* **38**, 467–491 (2010).
- Martin, S. *et al.* Kinematic and seismic analysis of giant tabular iceberg breakup at Cape Adare, Antarctica. *J. Geophys. Res.* **115**, B06311 (2010).
- Zoet, L. K., Anandakrishnan, S., Alley, R. B., Nyblade, A. A. & Wiens, D. A. Motion of an Antarctic glacier by repeated tidally modulated earthquakes. *Nature Geosci.* **5**, 623–626 (2012).
- Winberry, J. P., Anandakrishnan, S., Wiens, D. A. & Alley, R. B. Nucleation and seismic tremor associated with the glacial earthquakes of Whillans Ice Stream, Antarctica. *Geophys. Res. Lett.* **40**, 312–315 (2013).
- MacAyeal, D. R. *et al.* Transoceanic wave propagation links iceberg calving margins of Antarctica with storms in tropics and Northern Hemisphere. *Geophys. Res. Lett.* **33**, L17502 (2006).
- Brunt, K. M., Okal, E. A. & MacAyeal, D. R. Antarctic ice-shelf calving triggered by the Honshu earthquake and tsunami, March 2011. *J. Glaciol.* **57**, 785–788 (2011).
- Walker, C. C., Bassis, J. N., Fricker, H. A. & Czerwinski, R. J. Structural and environmental controls on Antarctic ice shelf rift propagation inferred from satellite monitoring. *J. Geophys. Res. Earth Surf.* **118**, 2354–2364 (2013).
- Peng, Z., Hill, D. P., Shelly, D. R. & Aiken, C. Remotely triggered microearthquakes and tremor in Central California following the 2010  $M_w$  8.8 Chile earthquake. *Geophys. Res. Lett.* **37**, L24312 (2010).
- Peng, Z. *et al.* Tectonic tremor beneath Cuba triggered by the  $M_w$  8.8 Maule and  $M_w$  9.0 Tohoku-Oki earthquakes. *Bull. Seismol. Soc. Am.* **103**, 595–560 (2013).
- Fry, B., Chao, K., Bannister, S. C., Peng, Z. & Wallace, L. Deep tremor in New Zealand triggered by the 2010  $M_w$  8.8 Chile earthquake. *Geophys. Res. Lett.* **38**, L15306 (2011).
- Velasco, A. A., Hernandez, S., Parsons, T. & Pankow, K. Global ubiquity of dynamic earthquake triggering. *Nature Geosci.* **1**, 375–379 (2008).
- Atlas of Antarctic Research, United States Antarctic Resource Center, United States Geological Survey, [http://gisdata.usgs.gov/website/antarctic\\_research\\_atlas/](http://gisdata.usgs.gov/website/antarctic_research_atlas/)
- Miyazawa, M. & Mori, J. Evidence suggesting fluid flow beneath Japan due to periodic seismic triggering from the 2004 Sumatra–Andaman earthquake. *Geophys. Res. Lett.* **33**, L05303 (2006).
- Rubinstein, J. L. *et al.* Seismic wave triggering of non-volcanic tremor, episodic tremor and slip, and earthquakes on Vancouver Island. *J. Geophys. Res.* **114**, B00A01 (2009).
- Walter, F. *et al.* Moment tensor inversions of icequakes on Gornergletscher, Switzerland. *Bull. Seismol. Soc. Am.* **99**, 852–870 (2009).
- Peng, Z. & Zhao, P. Migration of early aftershocks following the 2004 Parkfield earthquake. *Nature Geosci.* **2**, 877–881 (2009).
- Lough, A. C., Wiens, D. A., Barcheck, C. G. & Nyblade, A. Waveform studies of strong cryoseismic sources near the top of the Antarctic ice sheet. *AGU (Fall Meeting Suppl.)* abstr. C51B-0523 (2013).
- Lough, A. C. *et al.* Seismic detection of an active subglacial volcanic center in Marie Byrd Land, Antarctica. *Nature Geosci.* **6**, 1031–1035 (2013).
- Smith, A. M. Microearthquakes and subglacial conditions. *Geophys. Res. Lett.* **33**, L24501 (2006).
- Hill, D. P. Surface-wave potential for triggering tectonic (nonvolcanic) tremor—corrected. *Bull. Seismol. Soc. Am.* **102**, 2337–2355 (2012).
- Walter, J. I., Peng, Z., Tulaczyk, S. M., O’Neel, S. & Amundson, J. M. Triggering of glacier seismicity (Icequakes) by distant earthquakes. *Seismol. Res. Lett.* **84**, 372 (2013).
- Bindschadler, R. *et al.* The landsat image mosaic of Antarctica. *Remote Sens. Environ.* **112**, 4214–4226 (2008).
- Rignot, E., Mouginot, J. & Scheuchl, B. Ice flow of the Antarctic ice sheet. *Science* **333**, 1427–1430 (2011).
- Peng, Z., Long, L. T. & Zhao, P. The relevance of high-frequency analysis artifacts to remote triggering. *Seismol. Res. Lett.* **82**, 654–660 (2011).

## Acknowledgements

Financial support for this study was provided by the NSF CAREER grant EAR-0956051 (Z.P. and J.I.W.). POLENET-Antarctica is supported by NSF Office of Polar Programs grant numbers 0632230, 0632239, 0652322, 0632335, 0632136, 0632209, 0632185, and POLENET-Antarctica phase 2 is supported by NSF Office of Polar Programs grant numbers 1246776 1246712 and 1419268. Seismic instrumentation was provided and supported by the Incorporated Research Institutions for Seismology (IRIS) through the PASSCAL Instrument Center at New Mexico Tech. Seismic data are available through the IRIS Data Management Center. The facilities of the IRIS Consortium are supported by the NSF under Cooperative Agreement EAR-1063471, the NSF Office of Polar Programs and the DOE National Nuclear Security Administration. This manuscript benefits from useful comments by C. Aiken, F. Walter and C. Wu.

## Author contributions

Z.P. performed the analysis on detecting icequakes and statistical analysis of triggering potential. J.I.W. carried out the Rayleigh wave detector analysis. S.A., R.C.A., A.N. and D.A.W. led data collection efforts for POLENET seismic stations. All authors participated in interpreting the results and preparing the manuscript.

## Additional information

Supplementary information is available in the [online version of the paper](#). Reprints and permissions information is available online at [www.nature.com/reprints](http://www.nature.com/reprints). Correspondence and requests for materials should be addressed to Z.P.

## Competing financial interests

The authors declare no competing financial interests.